Derna Academy Journal for Applied Sciences

E-ISSN: 3006-3159

DAJAS

Numerical Optimization of a CZTS Thin-Film Solar Cell for Enhanced Photovoltaic Performance Using SCAPS-1D

Wafaa F. Gebril [1*]

[1]Department of Physics, Faculty of Science-Almarj, University of Benghazi, Almarj, Libya

*Corresponding author: E-mail address: gebrilwafaa@gmail.com

Volume: 7 **Issue: 2** **Page Number: 124 - 133**

Keywords:
CZTS; SCAPS-1D; thin-film solar cell; CdS; ZnO; ITO; photovoltaic performance.

Received: 15\08\2026
Accepted: 23\08\2026
Published: 24\08\2026

https://doi.org/10.71147/mh4m8873

ABSTRACT

Earth-abundant and non-toxic copper zinc tin sulfide (Cu2ZnSnS4, CZTS) serves as a compelling absorber candidate for thin-film solar technology, characterized by a favorable direct optical bandgap near 1.5 eV alongside a strong absorption coefficient. This work presents a numerical simulation of an ITO ZnO CdS CZTS Mo heterojunction configuration carried out via the SCAPS-1D platform under ambient conditions (300 K) and standard AM1.5G solar spectrum (100 mW cm^2). Key physical parameters, including the spatial dimensions of the CZTS absorber, ZnO window, and CdS buffer layers, alongside acceptor doping densities and working temperatures, were systematically varied to evaluate device characteristics. Findings demonstrate that increasing the CZTS absorber thickness enhances the photovoltaic response up to an optimum thickness of 2.4 µm, beyond which only a limited additional improvement is obtained. The ZnO thickness has a comparatively minor influence on the simulated performance over the investigated range; therefore, a thickness of 50 nm was selected as a practical value while maintaining near-maximum efficiency. The absorber acceptor concentration strongly affects the device characteristics, with an optimum practical value of NA=1×10^{18} cm^{-3} identified for the investigated structure. Following optimization of the selected device parameters, the proposed solar cell achieves a maximum power conversion efficiency of 24.19%, with an open-circuit voltage V_{oc} of 1.057 V, a short-circuit current density J_{sc} of 26.18 mA cm^{-2}, and a fill factor FF of 87.42%. These outcome metrics confirm that comprehensive physical and electrical calibration across the absorber, buffer, and window regions significantly boosts the simulated efficiency of thin-film CZTS heterojunction devices.

1. INTRODUCTION

Driven by the rising worldwide need for renewable and eco-friendly power, significant scientific focus has shifted toward photovoltaic systems capable of delivering cost-effective and high efficiency power generation (Haegel et al., 2019; Intal & Ebong, 2026). Solar energy has received particular attention because of its abundance, wide availability, and potential for long-term sustainable electricity generation (Armstrong et al., 2016; Sivula & van de Krol, 2016).

Among photovoltaic systems, thin-film architectures are attractive because they require relatively small amounts of active material, enable lightweight device structures, and offer the potential for low-cost, scalable fabrication (Intal & Ebong, 2026). Kesterite copper zinc tin sulfide (Cu_2ZnSnS_4, CZTS) has attracted considerable interest as a p-type absorber material owing to an optimal direct bandgap near 1.4 -1.5 eV and an elevated absorption coefficient exceeding 10 cm^{-1}) (Katagiri et al., 2009; Suryawanshi et al., 2013). In addition, CZTS consists of earth-abundant and relatively inexpensive elements, establishing a viable alternative to Cu (In, Ga) Se_2, which relies on costly, rare indium/gallium, and toxic CdTe systems (Katagiri et al., 2009; Intal & Ebong, 2026). These characteristics, together with its suitable optoelectronic properties, make CZTS a promising candidate for eco-friendly and potentially cost-effective thin-film photovoltaic applications (Katagiri et al., 2009; Suryawanshi et al., 2013). Despite these advantages, the performance characteristics of CZTS solar cells remain limited by several material and interface-related issues. Intrinsic defects, cation disorder, secondary phases, and non-radiative recombination can lead to significant voltage losses and limit the achievable device efficiency (Sahu et al., 2021; Kumar et al., 2015; Wei et al., 2023). Recombination at the absorber/buffer interface has also been identified as a major loss mechanism in kesterite photovoltaic devices (Siebentritt, 2013). These limitations can adversely affect the key photovoltaic performance parameters, namely V_{oc}, J_{sc}, FF, and PCE. A typical CZTS solar cell architecture employs a p-type CZTS absorber together with an n-type CdS buffer layer, a ZnO-based window layer, and a metallic back contact such as Mo (Katagiri et al., 2009). The thickness and electrical features of the individual layers can strongly influence photogeneration, drift-diffusion transport, recombination, and charge collection, and therefore directly impact the overall cell performance (Benzetta et al., 2021; Ait Abdelkadir & Sahal, 2023). Numerical simulation provides an efficient approach to investigating the electrical behavior of thin film solar cells and evaluating the influence of material and structural parameters before experimental fabrication. The Solar Cell Capacitance Simulator in One Dimension (SCAPS-1D) is a widely used numerical tool for modeling multilayer semiconductor solar cells and calculating characteristics such as current–voltage and capacitance responses (Burgelman et al., 2000). Previous numerical studies have demonstrated that the operation of CZTS solar cells is sensitive to variables such as absorber thickness, carrier densities, buffer-layer properties, and operating temperature (Ait Abdelkadir & Sahal, 2023; Belarbi et al., 2023; Benzetta et al., 2021). Recent SCAPS-1D investigations have examined the effects of the thickness of the CZTS absorber layer, carrier concentration, and operating temperature, demonstrating the importance of these parameters in determining device performance (Belarbi et al., 2023). However, the optimum values of these parameters depend on the selected device architecture, material properties, defect characteristics, and simulation conditions. In this work, a simulation study of an ITO/ZnO/CdS/CZTS/Mo heterojunction solar cell is performed utilizing the SCAPS-1D simulation software. The effects of absorber, buffer, and window layer thicknesses, absorber acceptor concentration (NA), and operating temperature (T) are systematically investigated. Their influence on the primary photovoltaic performance parameters, including V_{oc}, J_{sc}, FF, and PCE, is evaluated to determine suitable structural and operating conditions for improving the overall performance of the modeled CZTS device.

2. MATERIAL

The Schematic structure of the proposed thin-film solar device is shown in Figure 1. The photovoltaic performance of the solar cell was numerically evaluated using the one-dimensional Solar Cell Capacitance Simulator (SCAPS-1D) (Ait Abdelkadir & Sahal, 2023; Burgelman et al., 2000). Cadmium sulfide (CdS) was selected as the buffer layer because its n-type conductivity and suitable band alignment make it ideal for forming a p-n heterojunction with the p-type CZTS absorber layer (Katagiri et al., 2009; Belarbi et al., 2023). Zinc oxide (ZnO) was employed as the window layer owing to its wide bandgap, high optical transparency, and appropriate electrical properties, which allow incident light to reach the absorber while supporting carrier transport (Park et al., 2020; Katagiri et al., 2009). Indium tin oxide (ITO) was used as the front transparent conducting oxide (TCO) layer because of its high optical transmittance combined with superior electrical conductivity, providing effective light transmission and a low-resistance path for carrier extraction (Ellmer, 2012; Park et al., 2020). Finally, molybdenum (Mo) was selected as the back contact due to its suitable work function, high electrical conductivity, and chemical stability during CZTS processing. The Mo/CZTS interface can be affected by the formation of an interfacial molybdenum disulfide MoS_2 layer during sulfurization, which influences back contact resistance and overall solar cell performance (Scragg et al., 2012; Zhang et al., 2021).

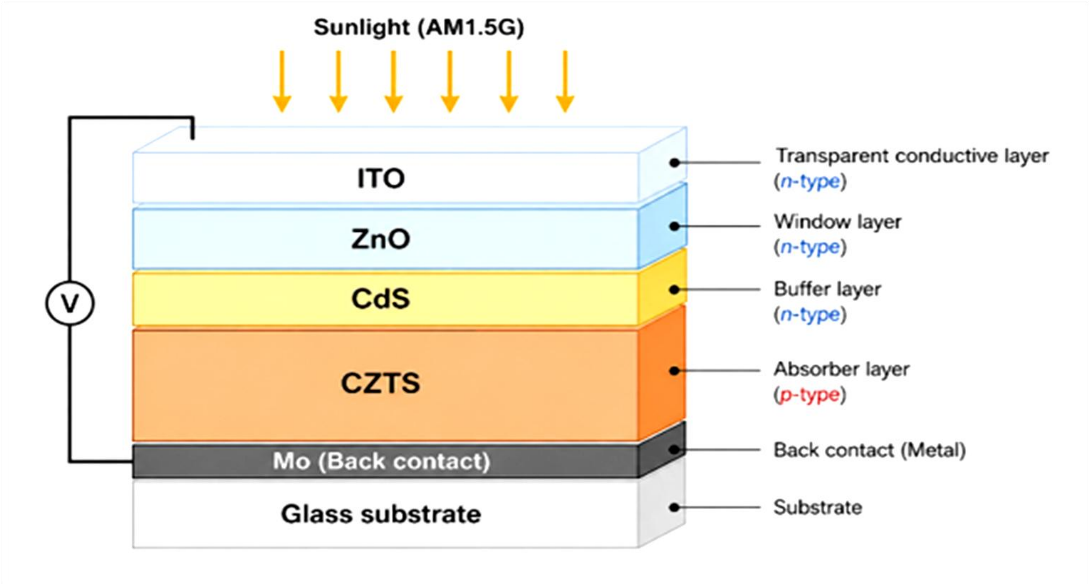

Figure 1: Schematic structure of the simulated ITO/ZnO/CdS/CZTS/Mo thin-film solar cell.

The physical parameters used in the simulation, including layer thicknesses, band gaps, electron affinities, and other relevant physical and electrical properties of the proposed solar cell layers, are summarized in Table 1 (Ranjan et al., 2023; Sultan et al., 2024; Lai & Lin, 2024).

3. ETHICS APPROVAL

Ethical approval was not required for this study because the research was entirely simulation-based and involved numerical modeling of a thin-film solar cell using the SCAPS-1D simulation software. No human participants, animals, human data, or biological materials were involved in the research.

Table 1: Physical parameters and material properties used in the SCAPS-1D simulation for the ITO/ZnO/CdS/CZTS/Mo solar cell layers.

Parameters	p-CZTS	n-CdS	n-ZnO	ITO
Thickness (nm)	500-5000	10-200	10-300	60
Bandgap (eV)	1.5	2.4	3.3	3.6
Electron affinity (eV)	4.5	4.5	4.6	4.1
Dielectric permittivity	9	9	9	10
CB effective density of states (cm^{-3})	2.2×10^{18}	2.2×10^{18}	2.2×10^{18}	2.2×10^{18}
VB effective density of states (cm^{-3})	1.8×10^{19}	1.8×10^{19}	1.8×10^{19}	1.8×10^{19}
Electron thermal velocity ($cm\ s^{-1}$)	1×10^{7}	1×10^{7}	1×10^{7}	1×10^{7}
Hole thermal velocity ($cm\ s^{-1}$)	1×10^{7}	1×10^{7}	1×10^{7}	1×10^{7}
Electron mobility (cm^2/V_s)	60	100	100	50
Hole mobility (cm^2/V_s)	20	25	25	75
Shallow donor density	-	1×10^{18}	1×10^{18}	1×10^{19}
Shallow acceptor density	1×10^{18}	-	-	-

3. Results

3.1 Performance Dependency on CdS Buffer Thickness

To evaluate the influence of the CdS layer thickness on the photovoltaic output metrics of the proposed device, its thickness was systematically swept from 10 to 300 nm. The resulting trends in V_{oc}, J_{sc}, FF, and PCE are presented in Figure 2. As the CdS buffer-layer thickness rises, V_{oc} exhibits only a minor increase, rising slightly from ~ 0.983 V to a saturated value of ~ 0.992 V above 60–80 nm. A similar behavior is seen for FF, increasing at lower CdS thicknesses before gradually reaching saturation. In contrast, J_{sc} exhibits a slight decrease with increasing CdS thickness, from approximately 27.47 to 27.40 mA cm^{-2}, which can be attributed to increased parasitic absorption within the CdS layer and the resulting reduction in the photon flux reaching the CZTS absorber. The combined variation of these photovoltaic parameters results in a maximum simulated efficiency of approximately 23.29% at a CdS thickness of about 86 nm. Beyond this thickness, efficiency changes only marginally and gradually decrease. Therefore, a CdS thickness of 80 nm was selected as the optimized value for the proposed device, as it provides performance very close to the maximum while avoiding unnecessary increases in buffer-layer thickness.

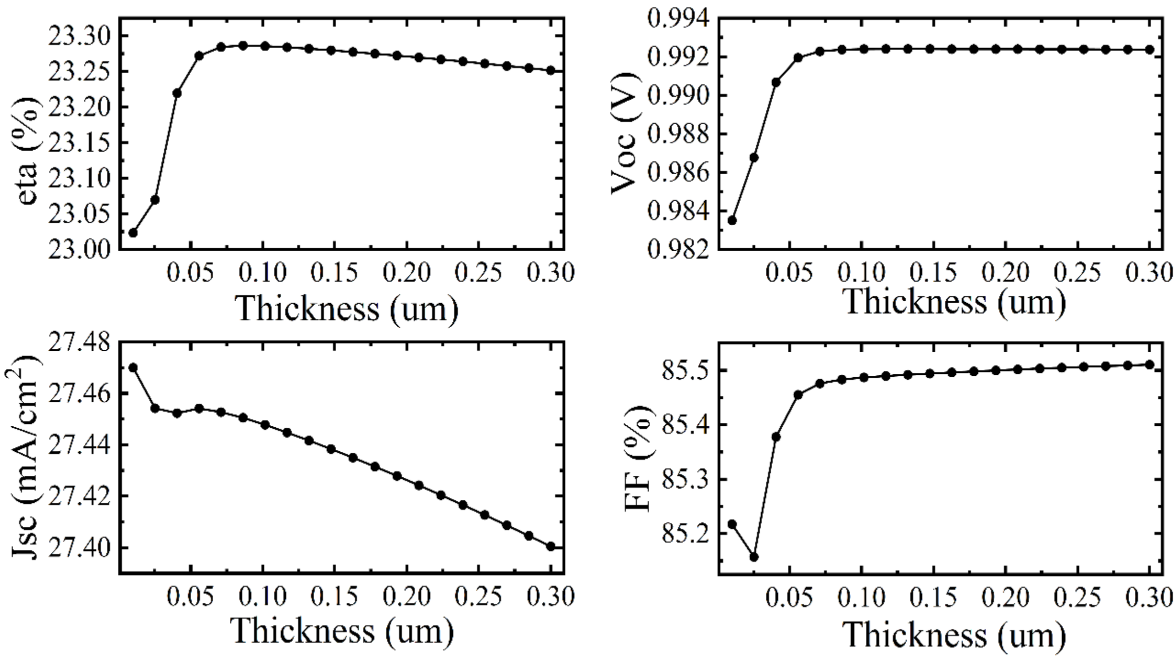

Figure 2: Effect of CdS buffer layer thickness on the photovoltaic performance parameters of the device.

3.2 Performance Dependency on ZnO Window Thickness

Figure 3 shows the impact of varying the ZnO window-layer thickness from 10 nm to 300 nm on the photovoltaic performance parameters of the proposed solar cell. Across the entire thickness range, J_{sc}, FF, and PCE exhibit only marginal variations. Specifically, J_{sc} undergoes a minor reduction from 27.47 mA cm^{-2} to 27.40 mA cm^{-2}, while FF remains virtually unchanged at approximately 85.5%. Consequently, power conversion efficiency drops negligibly from 23.30% at 10 nm to 23.25% at 300 nm. Meanwhile, the V_{oc} remains invariant at 0.992 V, as modifying the window layer thickness does not alter the built-in potential or junction band alignment of the absorber/buffer interface.

The subtle decrease in J_{sc} with increasing ZnO thickness is primarily attributed to parasitic ultraviolet absorption and mild transmittance attenuation within the window layer (Chen et al., 2024). Experimental studies have shown that ZnO thickness affects both the optical transmittance and photovoltaic performance of kesterite solar cells; moreover, an excessively thin ZnO layer may be insufficient to suppress leakage pathways, whereas excessive thickness can increase series resistance (Chen et al., 2024; Alhammadi et al., 2019). Considering the negligible trade-off in simulated photoelectric metrics alongside physical processing requirements, a ZnO thickness of 50 nm was selected as an optimal baseline to balance device efficiency with realistic thin-film fabrication constraints (Chen et al., 2024; Liu et al., 2019).

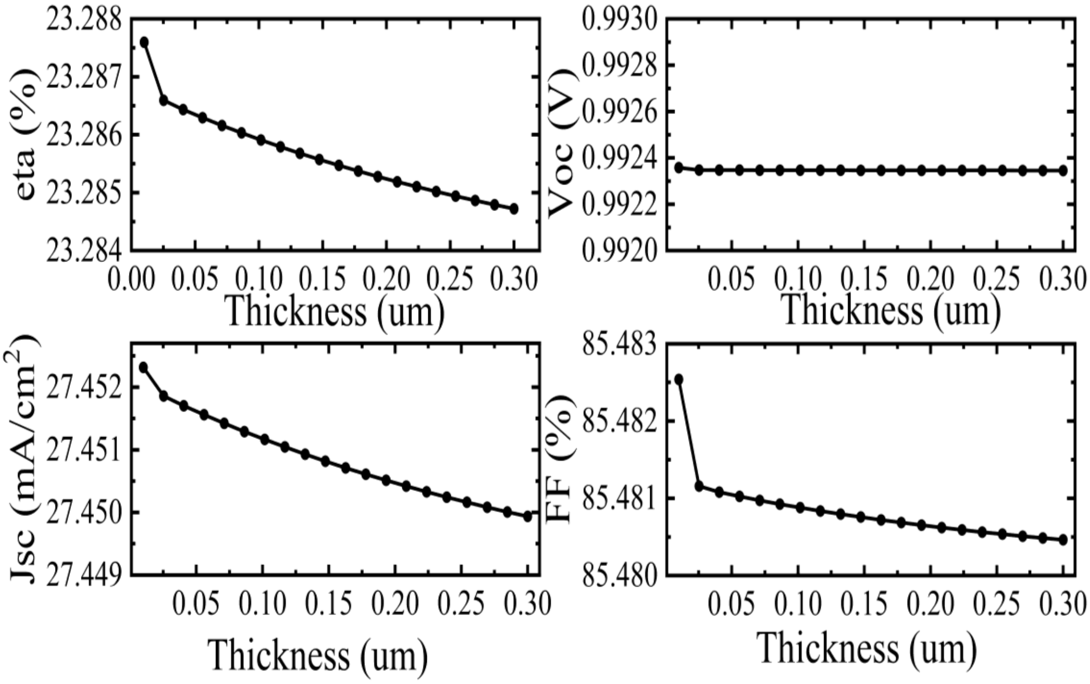

Figure 3: Influence of ZnO window layer thickness on the photovoltaic parameters of the proposed solar cell.

3.3 Performance Dependency on CZTS Absorber Thickness

The impact of the CZTS layer thickness on the photovoltaic performance of the proposed solar cell was investigated. The study evaluated an absorber layer thickness within 0.5 to 5.0 µm, while the CdS buffer layer and ZnO window layer thicknesses were fixed at 80 nm and 50 nm, respectively. Figure 4 presents the corresponding variations in device photovoltaic parameters as a function of absorber layer thickness. The results demonstrate that rising the CZTS thickness leads to a substantial improvement in performance at lower thickness levels. Specifically, the power conversion efficiency rises from 18.60% at 0.5 µm to 23.30% at 2.05 µm, accompanied by concurrent increases in J_{sc}, V_{oc}, and FF. This enhancement is mainly driven by increased optical absorption in the thicker CZTS layer, which elevates photogeneration and charge collection rates (Ait Abdelkadir & Sahal, 2023; Suryawanshi et al., 2013).

Beyond 2.05 µm, further increasing the absorber thickness yields diminishing performance gains. The efficiency increases modestly from 23.30% at 2.05 µm to 24.70% at 5.0 µm, with V_{oc} increasing from 0.993 V to 1.01 V, J_{sc} from 27.5 mA cm^{-2} to 28.3 mA cm^{-2}, and FF from 85.5% to 86.6%. This saturation behavior indicates that once the absorber thickness exceeds the effective optical absorption depth, additional material yields minimal photogeneration while slightly increasing bulk recombination resistance.

Based on these results, a CZTS layer thickness of 2.4 m was chosen as the optimal operating thickness for subsequent simulations. This value provides a strong performance profile with an efficiency of approximately 23.7% while avoiding unnecessary material consumption and processing complexity associated with thicker films.

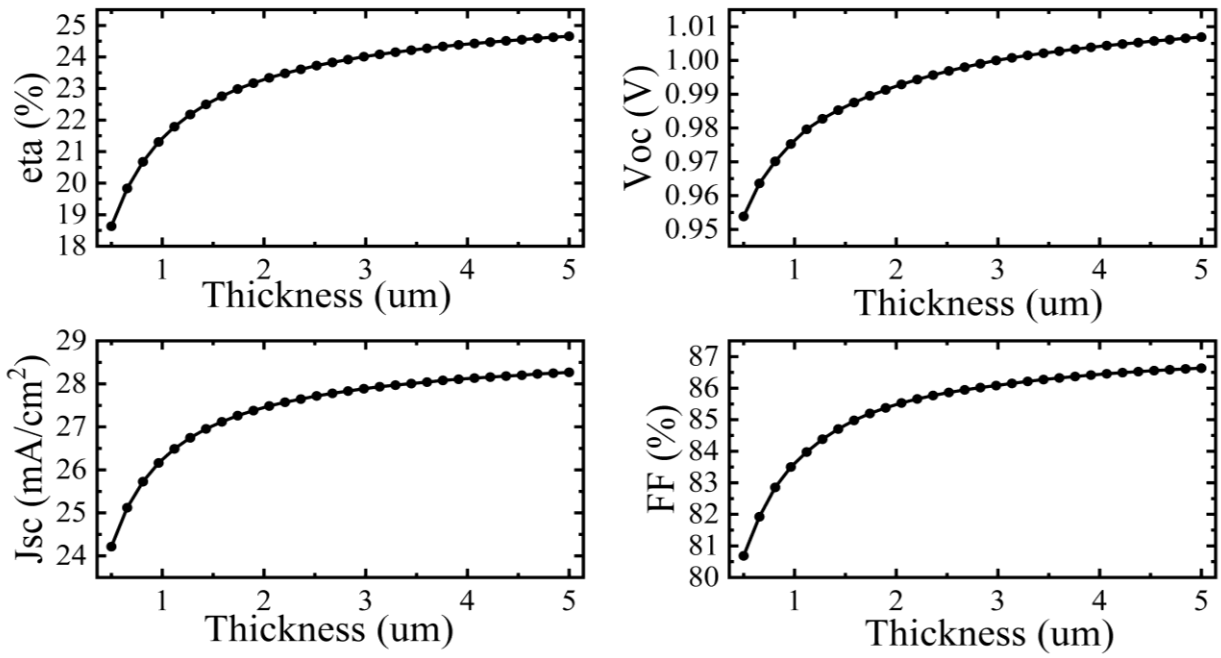

Figure 4: Variation of solar cell output parameters as a function of CZTS absorber layer thickness.

3.4 Effect of Acceptor Concentration on Device Performance

As illustrated in Figure 5, varying the acceptor concentration (N_A) of the CZTS absorber layer from 1×10^{14} cm^{-3} to 1×10^{19} cm^{-3} has a significant effect on the photovoltaic performance of the proposed solar cell. The power conversion efficiency (PCE) increases from 22.80% at $N_A = 3 \times 10^{14}$ cm^{-3} to 27.70% at 1×10^{19} cm^{-3}. A similar upward trend is observed in the V_{oc}, which rises from 0.928 V to 1.15 V over the investigated concentration range. This behavior is attributed to the increased majority carrier concentration, which enhances the built-in potential (V_{bi}) across the heterojunction and promotes charge separation and collection.

In contrast, the J_{sc} decreases gradually from 28.5 mA · cm^{-2} to 27.2 mA · cm^{-2} as the acceptor concentration increases, primarily due to the narrowing of the space-charge region. However, the FF improves steadily with higher acceptor doping, reaching 89.0% at 1×10^{19} cm^{-3} due to reduced bulk series resistance. The combined enhancements in V_{oc} and FF outweigh the minor reduction in J_{sc}, driving the overall increase in conversion efficiency.

Although the simulated efficiency continues to increase at concentrations above 1×10^{18} cm^{-3}, the value of $N_A = 1 \times 10^{18}$ cm^{-3} was selected as the practical operating doping density for the optimized device. At this concentration, the cell achieves an efficiency of 24.19%, a V_{oc} of 1.06 V, a J_{sc} of 27.2 mA · cm^{-2}, and an FF of 87.5%. Thus, 1×10^{18} cm^{-3} provides an optimal compromise between photovoltaic performance and physical doping feasibility while avoiding heavy-doping effects.

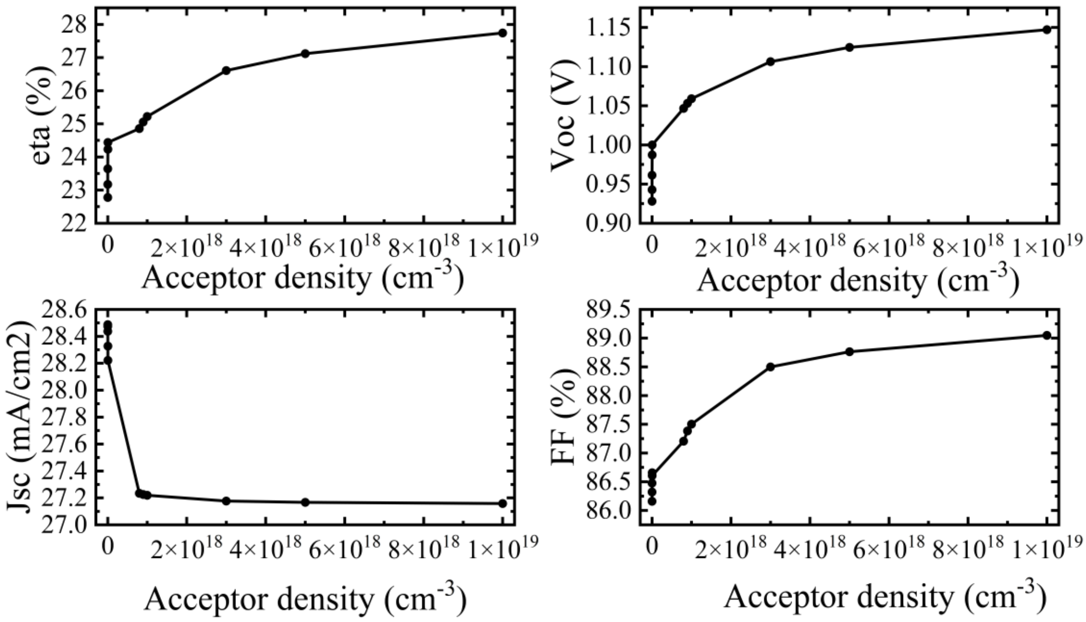

Figure 5: Impact of CZTS absorber acceptor concentration (N_A) on V_{oc}, J_{sc}, FF, and PCE.

3.5 Performance Dependency on Operating Temperature

To evaluate the thermal stability of the proposed solar cell, the operating temperature (T) was varied from 300 to 400 K. As shown in Figure 6, increasing the operating temperature results in a gradual decline in the photovoltaic performance of the device. The PCE decreases from 25.20% at 300 K to 19.65% at 400 K. This reduction is primarily associated with the decrease in the V_{oc}, which decreases from 1.06 V at 300 K to 0.876 V at 400 K. The corresponding average temperature coefficient of V_{oc} (dV_{oc}/dT) is approximately $-1.84\ \mathrm{mV \cdot K^{-1}}$. The reduction in V_{oc} with increasing temperature can be attributed to the thermally induced increase in carrier generation and recombination, which increases the reverse saturation current and consequently reduces the achievable photovoltage.

The FF also decreases progressively from 87.5% at 300 K to 82.4% at 400 K, indicating a deterioration in the electrical characteristics of the device at elevated temperatures. In contrast, the J_{sc} remains essentially constant at approximately $27.2\ \mathrm{mA \cdot cm^{-2}}$ throughout the investigated temperature range, indicating that temperature variation has only a minor effect on the photogenerated current. Overall, the results demonstrate that the thermal degradation of the proposed solar cell is primarily governed by the reductions in V_{oc} and FF, leading to a substantial decrease in conversion efficiency at elevated operating temperatures. These findings highlight the importance of effective thermal management for maintaining high photovoltaic performance under elevated-temperature operating conditions.

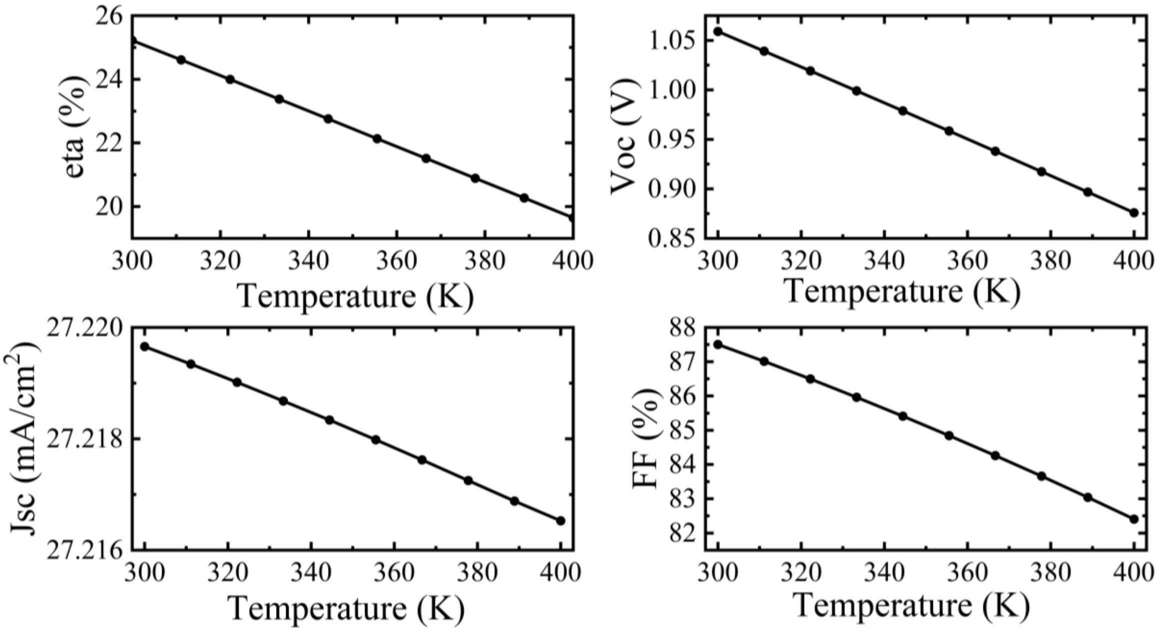

Figure 6: Temperature dependence of photovoltaic performance metrics in the range of 300 K to 400K.

Figure 7 shows the illuminated J-V curve for the fully optimized ITO/ZnO/CdS/CZTS/Mo solar cell under AM1.5G conditions (300 K). Using the optimized parameters ($t_{\mathrm{CZTS}} = 2.4\ \mu$m, $t_{\mathrm{CdS}} = 80$ nm, $t_{\mathrm{ZnO}} = 50$ nm, and $N_A = 1 \times 10^{18}$ cm^{-3}), the cell achieves a peak efficiency (PCE) of 24.19%, with $V_{oc} = 1.057$ V, $J_{sc} = 26.18$ mA $\cdot$ cm^{-2}, and FF $= 87.42\%$. These results confirm that balancing layer thicknesses and absorber doping effectively minimizes recombination and maximizes device performance.

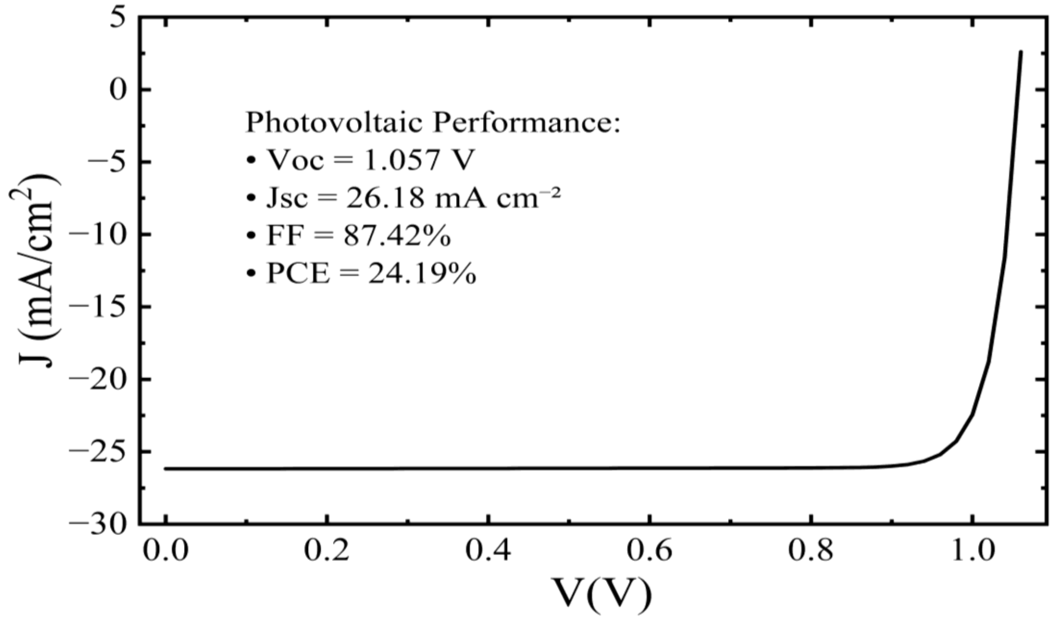

Figure 7: Illuminated J-V characteristic curve of the fully optimized ITO/ZnO/CdS/CZTS/Mo solar cell under standard AM1.5G conditions at 300K.

4. CONCLUSION

In this study, a numerical investigation of a ITO/ZnO/CdS/CZTS/Mo thin-film heterojunction solar cell was successfully performed using SCAPS-1D. The influence of absorber, buffer, and window layer dimensions, alongside absorber acceptor concentration (N_A) and working temperature, was systematically evaluated to determine optimal design parameters. The results demonstrate that increasing the CZTS absorber thickness enhances photon absorption and photogeneration up to an optimal thickness of 2.4 μm, beyond which efficiency increases at a significantly slower rate. For the buffer layer, a CdS thickness of 80 nm was selected to minimize parasitic absorption in the short-wavelength (blue) region while ensuring complete junction coverage. The ZnO window layer exhibited minimal impact on performance over the investigated range, with a thickness of 50 nm selected for practical fabrication continuity. Furthermore, optimizing the absorber acceptor concentration to $N_A = 1 \times 10^{18}$ cm^{-3} significantly enhanced the built-in potential and open-circuit voltage (V_{oc}), balancing charge extraction with heavy-doping constraints. Under these optimized conditions, the proposed solar cell achieves a maximum power conversion efficiency (PCE) of 24.19%, with $V_{oc} = 1.057$ V, $J_{sc} = 26.18$ mA $\cdot$ cm^{-2}, and FF = 87.42%. These findings provide critical design guidelines for fabricating high-performance, cost-effective CZTS-based photovoltaics.

7. REFERENCES

Ait Abdelkadir, A., & Sahal, M. (2023). Theoretical development of the CZTS thin-film solar cell by SCAPS-1D software based on experimental work. *Materials Science and Engineering: B*, 296, Article 116710. https://doi.org/10.1016/j.mseb.2023.116710

Alhammadi, S., Park, H., & Kim, W. K. (2019). Optimization of intrinsic ZnO thickness in Cu(In,Ga)Se_2-based thin film solar cells. *Materials*, 12(9), Article 1365. https://doi.org/10.3390/ma12091365

Armstrong, R. C., Wolfram, C., de Jong, K. P., Gross, R., Lewis, N. S., Boardman, B., ... Yano, J. (2016). The frontiers of energy. *Nature Energy*, 1, Article 15020. https://doi.org/10.1038/nenergy.2015.20

Belarbi, F., Matur, U. C., Tamin, C., Rahal, W., Benghabrit, S., Baydogan, N., & Adnane, M. (2023). Experimental study and numerical simulation for the development of critical performance parameters of eco-friendly Cu_2ZnSnS_4-based solar cells. *Optics & Laser Technology*, 158, Article 108800. https://doi.org/10.1016/j.optlastec.2022.108800

Benzetta, A. E., Abderrezek, M., & Djeghlal, M. E. (2021). Numerical study of CZTS/CZTSSe tandem thin film solar cell using SCAPS-1D. *Optik*, 242, Article 167320. https://doi.org/10.1016/j.ijleo.2021.167320

Burgelman, M., Nollet, P., & Degrave, S. (2000). Modelling polycrystalline semiconductor solar cells. *Thin Solid Films*, 361–362, 527–532. https://doi.org/10.1016/S0040-6090(99)00825-1

Chen, J., Xu, B., Ma, H., Tong, H., Zou, L., Yang, P., Chu, J., Sun, L., & Chen, Y. (2024). Enhanced the performance of CZTSSe solar cells by optimized i:ZnO window layer. *Materials Science in Semiconductor Processing*, 171, Article 107993. https://doi.org/10.1016/j.mssp.2023.107993

Ellmer, K. (2012). Past achievements and future challenges in the development of optically transparent electrodes. *Nature Photonics, 6*(12), 809–817. https://doi:10.1038/nphoton.2012.282

Haegel, N. M., Atwater, H., Barnes, T., Breyer, C., Burrell, A., Chiang, Y.-M., ... Glunz, S. (2019). Terawatt-scale photovoltaics: Transform global energy. *Science*, 364(6443), 836–838. https://doi.org/10.1126/science.aaw1845

Intal, D., & Ebong, A. U. (2026). Thin-film solar photovoltaics: Trends and future directions. *Renewable and Sustainable Energy Reviews*, 226, Article 116464. https://doi.org/10.1016/j.rser.2025.116464

Katagiri, H., Jimbo, K., Maw, W. S., Oishi, K., Yamazaki, M., Araki, H., & Takeuchi, A. (2009). Development of CZTS-based thin film solar cells. *Thin Solid Films*, 517(7), 2455–2460. https://doi.org/10.1016/j.tsf.2008.11.002.

Kumar, M., Dubey, A., Adhikari, N., Venkatesan, S., & Qiao, Q. (2015). Strategic review of secondary phases, defects and defect-complexes in kesterite CZTS–CZTSSe solar cells. *Energy & Environmental Science*, 8(11), 3134–3159. https://doi.org/10.1039/C5EE02153G

Lai, C.-K., & Lin, Y.-C. (2024). Numerical investigation and device architecture optimization of Sb_2Se_3 thin-film solar cells using SCAPS-1D. *Materials*, 17(24), Article 6203. https://doi.org/10.3390/ma17246203

Liu, B., Guo, J., Hao, R., Liu, X., et al. (2019). Effect of ZnO intermediate layer thickness on performance of Cu_2ZnSnS_4 solar cells. *Journal of Electronic Materials*, 48(8), 1–7. https://doi.org/10.1007/s11664-019-07284-6

Park, S. H., Crossay, A., & Naghavi, N. (2020). Transparent conductive oxides for thin film solar cells: Properties and applications. *IEEE Journal of Photovoltaics*, 10(3), 710–721. https://doi.org/10.1109/JPHOTOV.2020.2978120

Ranjan, R., Anand, N., Tripathi, M. N., Srivastava, N., Sharma, A. K., Yoshimura, M., Chang, L., & Tiwari, R. N. (2023). SCAPS study on the effect of various hole transport layer on highly efficient 31.86% eco-friendly CZTS based solar cell. *Scientific Reports*, 13, Article 18411. https://doi.org/10.1038/s41598-023-44845-6

Sahu, S., Bais, B., & Santhosh, M. (2021). Optimization of CZTS based solar cell using SCAPS-1D. *Optical and Quantum Electronics*, 53(10), Article 592. https://doi.org/10.1007/s11082-021-03225-8

Scragg, J. J., Wätjen, J. T., Edoff, M., Ericson, T., Kubart, T., & Platzer-Björkman, C. (2012). A detrimental reaction at the molybdenum back contact in $Cu_2ZnSn(S,Se)_4$ thin-film solar cells. *Journal of the American Chemical Society, 134*(47), 19330–19333. https://doi:10.1021/ja308862n

Siebentritt, S. (2013). Why are kesterite solar cells not 20% efficient? *Thin Solid Films*, 535, 1–4. https://doi.org/10.1016/j.tsf.2012.12.089

Sivula, K., & van de Krol, R. (2016). Semiconducting materials for photoelectrochemical energy conversion. *Nature Reviews Materials*, 1, Article 15010. https://doi.org/10.1038/natrevmats.2015.10

Sultan, M. Z., Shahriar, A., Tota, R., Howlader, M. N., Rodro, H. H., Akhy, M. J., & Rashik, M. A. A. (2024). Numerical study and optimization of CZTS-based thin-film solar cell structure with different novel buffer-layer materials using SCAPS-1D software. *Energy and Power Engineering*, 16(4), 179–195. https://doi.org/10.4236/epe.2024.164009

Suryawanshi, M. P., Agawane, G. L., Bhosale, S. M., Shin, S. W., Patil, P. S., Kim, J. H., & Moholkar, A. V. (2013). CZTS based thin film solar cells: A status review. *Materials Technology*, 28(1–2), 98–109. https://doi.org/10.1179/1753555712Y.0000000038

Wei, H., Li, Y., Cui, C., Wang, X., Shao, Z., Pang, S., & Cui, G. (2023). Defect suppression for high-efficiency kesterite CZTSSe solar cells: Advances and prospects. *Chemical Engineering Journal*, 462, Article 142121. https://doi.org/10.1016/j.cej.2023.142121

Zhang, S., Fan, L., Yao, D., Wu, J., Guo, H., Wang, H., & Zhang, Y. (2021). Band alignment tuning at Mo/CZTS back contact interface through surface oxidation states control of Mo substrate. *Solar Energy Materials and Solar Cells*, 229, Article 111141. https://doi.org/10.1016/j.solmat.2021.111141